

CO in blue compact and star burst galaxies

P.M. Gondhalekar¹, L.E.B. Johansson², N. Brosch³, I.S. Glass⁴, and E. Brinks⁵

¹ Rutherford Appleton Laboratory, Chilton, OXON, OX11 0QX, UK

² Chalmers University of Technology, Onsala Space Observatory, S-439 92 Onsala, Sweden

³ Department of Physics & Astronomy, Tel Aviv University, Tel Aviv, Israel

⁴ South African Astronomical Observatory, PO Box 9, Observatory 7935, Cape Town, South Africa

⁵ Departamento de Astronomia, Universidad de Guanajuato, Apdo. Postal 144, Guanajuato, Mexico

Received 16 February 1998 / Accepted 18 March 1998

Abstract. $^{12}\text{CO}(J=1\rightarrow 0)$ observations of 34 blue compact and star burst galaxies are presented. Although these galaxies are experiencing vigorous star formation at the current epoch, CO has been detected in only five of them. The five detections reported in this paper are all in galaxies with relatively red colours, $(B-V)_0 > 0.4$.

The new observations, when combined with previously published data on CO in BCGs, indicate that CO luminosity decreases with absolute luminosity of BCGs. Since the absolute luminosity of a galaxy is correlated with its metallicity, these results confirm that low metallicity BCGs have low abundances of CO gas. We also show that the star formation rate determined from the H_β luminosity is lower than that determined from the far infrared luminosity.

Key words: galaxies: compact – galaxies: ISM – galaxies: starburst – radio lines:ISM

1. Introduction

Blue Compact Galaxies (BCGs) are the smallest star-forming extragalactic objects and they are experiencing massive bursts of star formation at the current epoch. The dwarf BCGs lack the elaborate gas dynamics and spiral arms which trigger star formation in giant galaxies and the mechanism for star formation in these galaxies is still unidentified. An acceptable description of their nature and their evolution has also not yet emerged. The metal and dust deficiency of BCGs suggests that they are either young galaxies which have recently formed out of protogalactic gas clouds or that they experience intermittent bursts of star formation followed by periods of quiescence (Searle, Sargent & Bagnuolo 1972, Huchra 1977, Thuan et al. 1983, Gondhalekar et al. 1983, 1986)

Observations of CO in nearby galaxies (Talbot 1980, Scoville & Young 1983) suggest that the formation of stars depends primarily on the availability of molecular gas. Thus observations of molecular gas in BCGs are essential to both the understanding of star-formation within them as well as their overall evolution.

CO observations of BCGs have been reported by Young et al. (1986), Israel & Burton (1986), Tacconi & Young (1987), Arnault et al. (1988), Sage et al. (1992) and Israel, Tacconi & Baas (1995). Various criteria were used to select the samples of galaxies observed in these studies. The consensus seems to be that *metal-poor galaxies are deficient in CO*. The current programme was initiated to explore the validity of this conclusion. A sample of galaxies, covering a large range in absolute magnitude and $60\mu\text{m}$ luminosity, has been observed in order to determine the CO content in the galaxies experiencing different levels of star bursts and spanning a range of metallicities. We should like to emphasise that we are unable to determine the molecular content of these galaxies from the CO observations as the CO-to- H_2 conversion factor is not known for the galaxies in this sample as the metallicity of these galaxies is not known and the conversion factor is a function of metallicity of a galaxy.

The sample of galaxies, the CO observations and the data reduction are described in Sect. 2. In Sect. 3 we investigate the relation between star-formation and CO in these galaxies. The conclusions are given in Sect. 4.

2. Sample, observations and data reduction

For this study a sample of galaxies covering a large range in luminosity and therefore, metallicity, was selected from the list of Salzer, MacAlpine and Boroson (1989). We have selected 13 galaxies classified as *dwarf HII hotspot galaxies, DHIIH*, by these authors. To this we have added a sample of nine *star burst nuclei, SBN*, (Salzer, MacAlpine and Boroson, 1989). The galaxies in both samples have H_β luminosity greater than 10^{38} erg s^{-1} ($H_0=75$ km s^{-1} Mpc $^{-1}$ and $q_0=0.5$ have been used through out this paper) and all are experiencing vigorous star bursts at the current epoch. Additional star burst galaxies, mainly from MacAlpine, Smith & Lewis (1977a,b) and MacAlpine & Lewis (1978) were added to this list. The full list of galaxies observed is given in Table 1. In total, 34 galaxies were observed. The sample covers about 6^m in absolute luminosity. This is not a complete sample, it is, however, a large sample and the number of BCGs is large enough to be representative as a class.

The observations of the $^{12}\text{CO}(J=1\rightarrow 0)$ (115.271 GHz) line were performed at the Onsala Space Observatory (OSO) 20m

Send offprint requests to: P.M. Gondhalekar

mm-wave telescope, the half-power beamwidth of which is $35''$ at this frequency. The observations were made during three runs between February 1995 and March 1997. A SIS mixer was used, tuned to the single side-band mode. Typical system temperatures, corrected for rearward

spillover and atmospheric attenuation, were between 500 K and 1500 K depending on weather conditions and galaxy redshifts. The back-end was a multichannel receiver with a resolution of 1 MHz and a total bandwidth of 512 MHz (corresponding to a velocity coverage of about 1300 km s^{-1} at 115 GHz) Antenna pointing was about $3''$ rms on each axis and the main-beam efficiency was $\eta_{mb}=0.5$ during all three observing runs. The observed intensities, T_a^* , were “chopper-wheel” calibrated and are related to the main-beam brightness temperature T_{mb} by $T_a^*=\eta_{mb}\times T_{mb}$.

The detections and the upper limits of CO for all galaxies are given in Table 1, where the rms error (Col.7) is calculated for a resolution of 20 km s^{-1} . This resolution seems to give the best signal-to-noise for the detected line widths. The intensity scale is the main beam brightness temperature T_{mb} . The integrated CO intensity $I_{CO} = \int T_{mb}dV$ is given in Col. (11). The 1σ error in the integrated line intensity, where the line has been detected, is given in Col. (12) and was calculated using Eq. (1) of Elfhag et al. (1996). These errors depend on the inherent rms noise in the profile and the uncertainties in baseline corrections. However, for most of the detected lines the baseline range is small and only the rms noise defines the error. This is, however, not true in cases where only upper limits can be determined, because in such cases the full spectrum defines the baseline range and the curvature of the baseline is included in computing the upper limits.

Of the 34 galaxies observed, CO was detected in five and there may be possible detection in three other cases. These eight spectra are shown in Fig. 1. In the following discussion the possible detections are regarded as upper limits.

Some galaxies in this sample (see Table 1) are AGNs. Only upper limits have been obtained for CO in these galaxies. These limits have been included in the following analysis but they do not affect our conclusions.

2.1. Comparison with previous observations

Tacconi & Young (1987) and Sage et al. (1992) have previously observed this CO line in II Zw 40. A comparison of the measurements, taking into account the different beam areas, suggests that the present observations are 0.21 dex higher than those of Tacconi & Young (1987) and 0.35 dex higher than those of Sage et al. (1992). However, the centroid velocity of the present observations is $\approx 645 \text{ km s}^{-1}$ while Tacconi & Young measure a velocity of $\approx 850 \text{ km s}^{-1}$ and Sage et al. a value of $\approx 770 \text{ km s}^{-1}$ respectively. Brinks & Klein (1988) have mapped II Zw 40 in HI with the VLA and they measured velocities between 750 and 800 km s^{-1} . The poor agreement between the velocity derived from our CO observations and the velocities seen in the VLA maps suggests a false detection of CO in the current observations.

Similarly, Taylor, Kobulnicky & Skillman (priv. comm.) have reported CO observations of UM477. The luminosity derived from the current observations is 0.42 dex higher than that observed by Taylor, Kobulnicky & Skillman, but the velocity from the current observations is in good agreement with the velocity of 1318 km s^{-1} obtained by these authors.

3. Star formation in blue compact and star burst galaxies

In this section we investigate the correlations between the CO luminosities and the absolute magnitudes, H_β luminosities, masses of neutral gas, far infrared (FIR) luminosities and the temperatures of dust in the blue compact and star burst galaxies in this sample. For completeness we have included (where possible) both detections and upper limits. The CO luminosity in the observed $35''$ region of each galaxy was calculated assuming $L_{CO} = (\pi r^2)I_{CO} (\text{K km s}^{-1} \text{ pc}^2)$ where r is the radius of the $35''$ beam on the galaxy in pc. The true CO luminosities may be somewhat higher since the complete galaxy was not included in the $35''$ beam in every case.

The luminosities of the galaxies which were detected are given in Table 2 and the upper limits are given in Table 3. In Table 2 we have also collated the observations of CO in BCGs made by Sage et al. (1992) and those by Taylor, Kobulnicky & Skillman (priv. com.). In these tables we have included the absolute magnitudes, the FIR luminosities and the HI masses. For consistency the absolute magnitudes (in Tables 2 and 3) and the HI masses (in Table 2), were obtained from the LEDA compilation (Paturel et al. 1997). Similarly the FIR luminosities for all galaxies were obtained from Salzer & MacAlpine (1988) (these are co-added IRAS survey data) where available and from the LEDA compilation otherwise. The FIR colour in Tables 2 and 3 is defined as $\log(f_{100}/f_{60})$ where f_{100} and f_{60} are the FIR flux densities at $100\mu\text{m}$ and $60\mu\text{m}$ respectively. These fluxes were also obtained from Salzer & MacAlpine (1988) where available and from the IRAS Point Source Catalogue (Lonsdale et al. 1985) otherwise. The uncertainty in the f_{100} and f_{60} flux densities is between 5% and 15%; corresponding to a maximum error of 20% in the ratio f_{100}/f_{60} .

In comparing the CO luminosities with HI masses and the FIR luminosities the differences in the apertures with which these observations were made should be borne in mind. The CO observations were made with a $35''$ field-of-view and the CO luminosities given in Tables 2 and 3 correspond only to the parts of the galaxies that were actually observed. The FIR observations (from the IRAS satellite) were made with apertures of $1.5'$ and $3.0'$ at $60\mu\text{m}$ and $100\mu\text{m}$ respectively, and the FIR luminosities of the complete galaxies will have been observed in all cases. Similarly, the HI observations have been made with a field-of-view larger than $35''$ in most cases.

The H_β luminosities given in Tables 2 and 3 were obtained from the equivalent widths of the H_β lines and the B-magnitudes given by Salzer, MacAlpine & Boroson (1989) and Terlevich et al. (1991) respectively. The equivalent width of the H_β line is obtained from spectroscopic observations made with a narrow slit and it is very likely that the slit was positioned on the

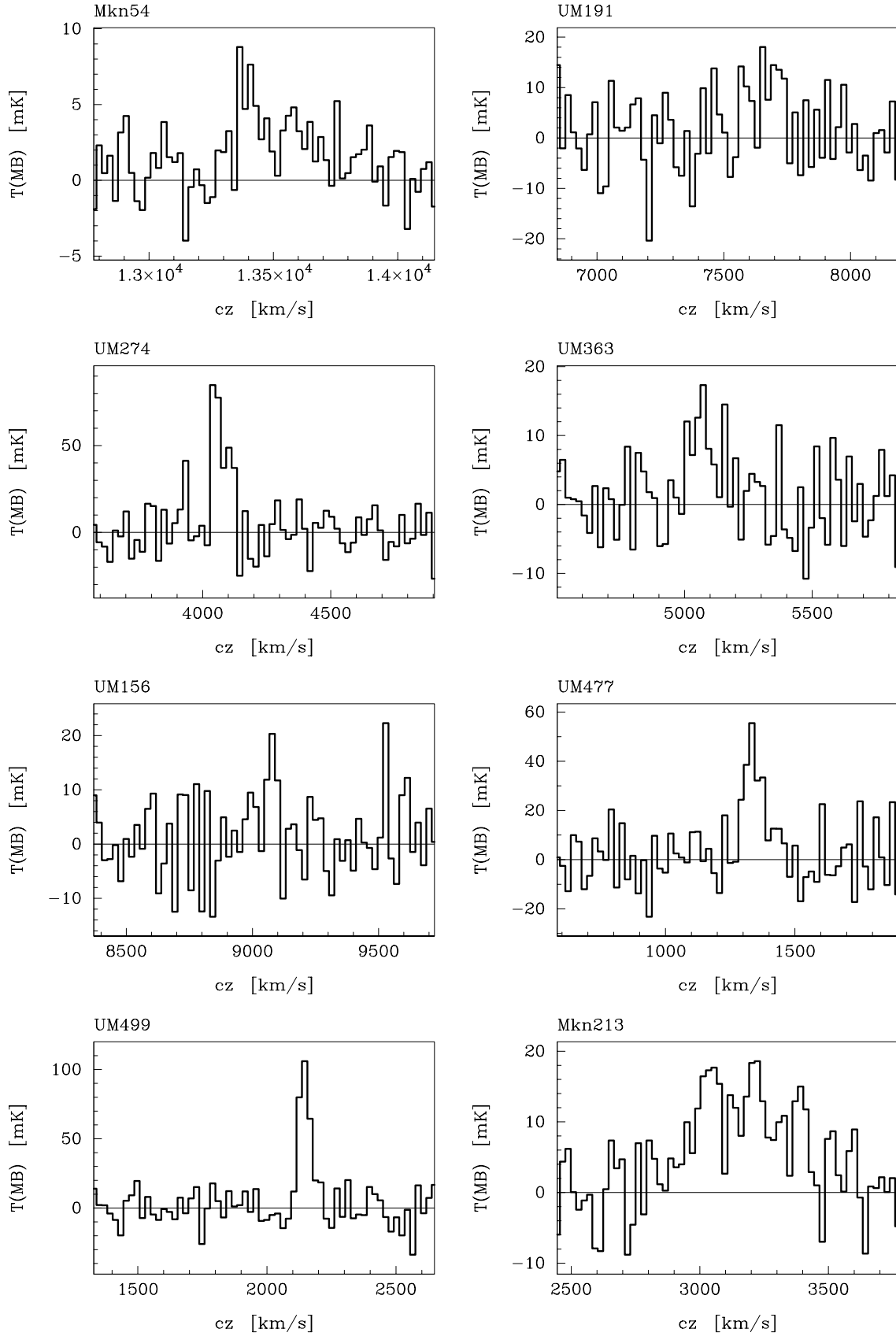


Fig. 1. CO spectra of eight star burst galaxies in the current sample. The intensity scales are in T_{mb} (mK). The velocities are cz (km s^{-1}) and have not been corrected for the solar motion or the Virgo-centric motion. The spectra have been smoothed to 20 km s^{-1} . Note that the detections of UM191, UM363 and UM156 are only tentative.

Table 1. ^{12}CO in bluse compact and star burst galaxies

ID			RA(1950)		Dec(1950)		(B-V) $_{cor}$	T_{mb}	σ_{mb}	$c \times z$	FWHW	I_{CO}	σ_{CO}		
1	2	3	4		5		6	7	8	9	10	11	12		
								mK	mK	km s $^{-1}$	km s $^{-1}$	K km s $^{-1}$			
UM274		Sb	0	43	32	-1	59	41	76	12.	4065	65	5.4	0.7	
UM286			0	49	26	-0	45	31	0.53	13.			<0.8		
UM307	SBd	SBN	1	08	56	1	03	24	0.41	4.8			<0.3		
UM323		DHIIIH	1	24	12	-0	54	15	0.40	11.			<0.6		
UM334		DHIIIH	1	30	05	-1	54	15	0.33	6.2			<0.4		
UM343	SBb	SBN	1	33	25	0	24	29	0.78	8.6			<0.5		
UM351		DHIIIH	1	35	48	1	38	48	0.56	4.9			<0.3		
UM363	SO-a	Sy 2	1	41	22	2	05	56	1.03	13	4.3	5070	125	1.7*	0.3
UM374		DHIIIH	1	50	20	-1	08	52	0.60	8.1			<0.5		
UM385		Sy 1	1	57	16	0	09	09		6.8			<0.3		
UM388		SBN	1	58	18	-1	46	50	0.72	4.6			<0.3		
UM393	SO	Sy 1	2	03	43	-0	31	46		5.7			<0.3		
UM413		SBN	2	12	21	2	00	47	0.75	3.4			<0.2		
UM418	SBb	SBN	2	17	07	-0	29	09		6.8			<0.4		
IIZw40	Sbc		5	53	05	3	23	05	0.82	23	6.6	645	45	1.1*	0.5
IZw18			9	30	30	55	27	49	0.10		4.8		<0.3		
UM439		DHIIIH	11	34	02	1	05	38	0.28		8.3		<0.5		
UM444		DHIIIH	11	37	38	-0	08	03	0.65		4.9		<0.3		
UM452	SO	DHIIIH	11	44	26	-0	00	57	0.64		13.		<0.7		
UM454		DHIIIH	11	45	43	-1	21	43	0.43		13.		<0.8		
UM456		DHIIIH	11	48	01	-0	17	23	0.35		11.		<0.7		
UM462		DHIIIH	11	50	03	-2	11	26	0.24		7.4		<0.5		
UM471		DHIIIH	11	58	56	-1	09	28	0.22		10.		<0.5		
UM477	SBc	SBN	12	05	36	3	09	21	0.62	50	8.6	1340	85	4.5	0.6
UM483		DHIIIH	12	09	41	0	21	00	0.02		14.		<0.8		
UM491		DHIIIH	12	17	18	2	03	02	0.42		14.		<0.8		
UM499	SO-a	SBN	12	23	09	0	50	57	0.64	110	10.	2145	55	6.2	0.5
Mark213	SBa		12	29	01	58	14	20	0.48	15	4.6	3160	360	5.4	0.5
Mark54	Sc		12	54	32	32	43	07	0.27	4	1.8	13500	430	1.5	0.2
UM530		SBN	12	55	35	2	07	54	0.51		5.8		<0.3		
UM549		DHIIIH	13	11	58	2	49	44	0.39		5.2		<0.3		
UM641	Sc	SBN	14	07	21	-1	00	15	0.43		5.0		<0.3		
UM156	Sb	Sy 1	23	16	23	-0	01	50		15	6.0	9080	65	1.0*	0.4
UM191	Im		23	54	26	-2	21	44		13	5.7	7675	150	2.0*	0.4

Column 2: Galaxy type; LEDA catalogue (Paturel et al. 1997)
Column 3: Galaxy type; Salzer et al. (1989)
(B-V) $_{cor}$ From Salzer et al. (1989), where available, and from the LEDA catalogue otherwise
Column 11: An asterisk denotes a possible detection only

brightest HII region in each galaxy in which these could be resolved. In using the equivalent width obtained from a narrow slit observation to obtain the luminosity of the entire galaxy we are assuming that the H_{β} surface brightness of the galaxy is similar to that of the region where the slit observations were made. This is unlikely to be true for all galaxies, particularly the non-compact galaxies. The H_{β} luminosities were corrected for extinction with the Galactic extinction law and the reddening coefficients given by Salzer, MacAlpine & Boroson (1989) and Terlevich et al. (1991).

3.1. CO–Absolute Magnitude correlation

The absolute magnitude of a galaxy is an indicator of its total stellar population, including as it does both the young stars in a starburst and the underlying older stars. Also, through the mass luminosity relation, the absolute magnitude is indicative of the total stellar mass of a galaxy. The correlation between the CO luminosity and the absolute magnitude of the galaxies in these samples is shown in Fig. 2a. In this sample of 34 galaxies, 14 galaxies are (equal to or) less luminous than $M_{abs} = -18$ (BCGs) and 20 are more luminous than $M_{abs} = -18$ (giants). CO has been detected in only 5 giants i.e. $\sim 25\%$ and not in any of the dwarfs. These observations of a large sample of BCGs confirm previous observations that BCGs are deficient in CO gas.

Table 2. CO and FIR luminosities and the HI mass in galaxies with CO detection

ID	m_B	M_B	z	$\log(L_{H\beta})$ erg s $^{-1}$	$\log(L_{FIR})$ L_{\odot}	C_{FIR}	$\log(L_{CO})$ K km s $^{-1}$ pc 2	$\log(M_{HI})$ M_{\odot}	D_{25} "
1	2	3	4	5	6	7	8	9	10
Mark54	15.29	-21.81	0.0447		10.69	-0.289	9.70		40
UM274	12.81	-21.22	0.1412	41.29	12.30	0.363	9.16	11.61	75
UM477	11.58	-19.85	0.0042	42.06	9.46	0.263	8.10	9.90	256
UM499	13.16	-19.40	0.0067	41.74	9.71	0.119	8.65	8.92	128
Mark213	13.10	-20.96	0.0104	39.86	10.05	0.242	8.95	9.31	97
T NGC1569	10.68	-20.15	-0.0005		8.51	0.039	5.25	8.04	
T NGC4214	10.13	-17.32	0.0010		8.61	0.240	5.96	9.05	
T NGC5253	10.77	-16.23	0.0010	41.16	8.86	-0.027	5.83	8.15	
UM465	13.96	-17.01	0.0034	41.19	8.45	0.115	6.28	7.59	
NGC6822	9.32	-17.55	0.0001		6.52	0.169	4.48	7.90	
He2-10	12.46	-18.78	0.0022		9.44	0.033	7.56	8.70	
S IIZw40	15.48	-16.15	0.0026	40.75	8.99	-0.056	6.81	8.37	
S Haro2	12.97	-19.07	0.0051		9.45	0.045	7.36	8.68	
S Haro3	13.21	-18.19	0.0034		8.75	0.742	7.52	8.75	
S Mark900	13.98	-17.50	0.0038				6.30	8.93	
S Mark86	12.19	-16.70	0.0015		8.31	0.298	6.18	8.28	
S UM456	15.21	-16.72	0.0056	41.09	8.28	0.260	7.32	8.52	
S UM462	14.56	-16.33	0.0034	40.52	8.42	0.030	7.51	8.15	
S Mark297	13.44	-21.19	0.0157		10.63	0.147	9.53	10.06	
S UM448	14.39	-20.39	0.0182	42.04	10.49	0.114	9.33	9.67	
column 7	FIR colour, $C_{FIR} = \log(f_{100}/f_{60})$								
T	Data from Taylor, Kobulnicky & Skillman (priv. com.)								
S	Data from Sage et al. 1992								
UM465	Data from Taylor et al. (1995)								
NGC6822	Data from Davies (1972)								
He2-10	Data from Kobulnicky et al. (1995)								

As already mentioned it is possible that the 35'' beam of OSO does not detect the total CO content of some galaxies as their optical sizes, judged from their D_{25} diameters (Table 2), are considerably larger than 35''. To check whether the CO luminosities of some of the galaxies in Table 2 may have been significantly under-estimated, we have included the observations of Young et al. (1986) in Fig. 2a. These authors have mapped CO in their sample of galaxies. In Fig. 2a, the data of Young et al. and the data of Sage et al. (1992) and Taylor, Kobulnicky & Skillman (priv. com.) are linearly correlated with M_{abs} and the present data are consistent with this correlation. A straight line fit to all data (both detections and upper limits, but excluding the data for NGC1569 and NGC6822) has the form;

$$\log(L_{CO}) = -1.96 \pm 0.83 + (-0.51 \pm 0.04) \times M_{abs}$$

with a Spearman's rho correlation coefficient of -0.81 (ASURV software of Isobe, LaValley & Feigelson STAR-LINK SUN/13.2, MUD/005) The two discrepant points are for NGC1569 and NGC6822 (Taylor, Kobulnicky & Skillman priv. com.). The D_{25} diameters of these two galaxies are 45'' and 151'' respectively and it is not clear why the CO luminosities of these galaxies are lower than the luminosities of other galaxies of comparable absolute magnitude.

This strong correlation between the CO luminosities and the absolute magnitudes of these galaxies suggests that the CO content of a galaxy is either determined by or depends on its total stellar content. It is also possible that the CO - M_{abs} correlation actually conceals the CO - metallicity correlation via the relation $\log(O/H)+12 = -0.2M_{abs}+4.86$ (Arimoto, Sofue & Tsujimoto (1996), Roberts & Haynes (1994), Wilson (1995)). It is not possible to confirm this possibility as metallicity data for the galaxies in the current sample are not available. The correlation in Fig. 2a. thus suggests that the CO luminosity of a galaxy is a tracer of either the total stellar mass or the metallicity of a galaxy.

The galaxies in this sample with detected CO are relatively red; the mean $(B-V)_{cor} = 0.5$. This is in disagreement with the observations of Israel, Tacconi & Baas (1995) whose observations of dwarf galaxies suggests that CO is preferentially detected in blue (dwarf) galaxies.

3.2. CO - H_{β} correlation

The H_{β} luminosity of a galaxy is proportional to the number of high mass stars in the galaxy, allowing for extinction and

Table 3. Upper limits of CO luminosities

ID	m_B	M_B	z	$\log(L_{H\beta})$ erg s ⁻¹	$\log(L_{FIR})$ L_{\odot}	C_{FIR}	$\log(L_{CO})$ K km s ⁻¹ pc ²
1	2	3	4	5	6	7	8
UM286	15.2	-16.68	0.0037				7.20
UM323	16.1	-17.22	0.0064	40.34	8.49	0.37	7.55
UM334	17.2	-16.98	0.0163	39.98	9.51	0.12	8.19
UM351	18.2	-16.91	0.0250	40.53	9.62		8.43
UM363	13.6	-20.96	0.0170	41.69	9.90	-0.005	8.85
UM374	17.6	-17.32	0.0191	40.87	9.48	0.36	8.42
UM385	15.7	-23.30	0.1629		12.43		10.06
UM393	14.4	-22.22	0.0424		10.14		8.89
UM418	14.2	-21.27	0.0253		10.54		8.57
IZw18	15.6	-15.18	0.0025				6.44
UM439	15.3	-16.45	0.0037	39.99	8.49	0.49	7.00
UM444	16.7	-19.00	0.0219	41.50	9.56		8.32
UM452	15.5	-16.45	0.0046	39.35	8.53	0.80	7.33
UM454	16.5	-17.68	0.0126	40.03	9.17	0.45	8.26
UM456	15.5	-16.72	0.0056	41.09	8.43	0.26	7.50
UM462	14.6	-16.33	0.0034	40.52	8.59	0.03	6.92
UM471	18.2	-17.98	0.0351	41.07	9.97		8.95
UM483	15.9	-17.12	0.0075	40.54	8.41		7.81
UM491	15.8	-16.39	0.0063	42.09	8.51	0.42	7.66
UM549	16.6	-18.08	0.0193	41.03	9.23		8.21
UM307	14.4	-21.07	0.0228	42.05	10.48	0.32	8.35
UM343	14.1	-20.78	0.0173	41.83	10.25	0.26	8.34
UM388	17.7	-21.63	0.1243	41.78	11.36	0.62	9.83
UM413	17.6	-20.97	0.0263	40.81	11.17	0.30	8.30
UM530	16.8	-20.93	0.0665	42.09	11.06	0.12	9.28
UM641	15.2	-20.33	0.0240	42.28	10.00	0.26	8.40
UM156	13.5	-22.43	0.0293	42.02	10.34	0.41	9.12
UM191	15.3	-19.87	0.2451				9.27

column 7 FIR colour, $C_{FIR}=\log(f_{100}/f_{60})$
column 8 Upper limit of CO luminosity

geometric factors (like the covering factor). The star-formation rate of the high mass stars is given by (Condon 1992)

$$\left[\frac{SFR(M \geq 5M_{\odot})}{M_{\odot} \text{yr}^{-1}}\right] \sim 6 \times 10^{-42} \eta^{-1} L_{H\beta}$$

where $L_{H\beta}$ is the dereddened H_{β} luminosity of a galaxy (in erg s⁻¹) and η is the covering factor. These high mass stars will only be a few million years old and will still be associated with the giant molecular clouds from which they formed. The CO – H_{β} correlation thus provides a link between the molecular clouds in a galaxy and the population of the high mass stars which form from these clouds.

In Fig. 2b the CO luminosity is shown as a function of the H_{β} luminosity. Both the CO detections and upper limits have been plotted along with the data of Sage et al. (1992) and those of Taylor, Kobulnicky & Skillman (priv. com.). The H_{β} luminosities in Fig. 2b suggest a SFR of $\sim 2 \times 10^{-2} M_{\odot} \text{yr}^{-1}$ to $\sim 6 M_{\odot} \text{yr}^{-1}$. These SFRs have been obtained for a covering factor $\eta = 1.0$, this is unlikely to be the case for all galaxies in this sample.

A straight line fit to all data in Fig. 2b. (i.e. both detections and upper limits) has the form;

$$\log(L_{CO}) = (-14.02 \pm 16.44) + (0.51 \pm 0.39) \times \log(L_{H\beta})$$

with a Spearman's rho correlation coefficient of 0.16 i.e. there is no correlation between the CO and H_{β} luminosities. These data suggest that the SFR, as obtained from the H_{β} luminosity of these galaxies, is independent of the CO content of these galaxies. It is possible that the assumption that the covering factor $\eta=1.0$ for all our galaxies is wrong and that it may in fact be a function of the SFR; i.e. as the SFR increases, the wind and the supernovae will disperse the surrounding gas and decrease the covering factor.

3.3. CO-HI correlation

In order to investigate the relation between the CO and atomic gas contents of blue compact and star burst galaxies, the CO luminosity is plotted as a function of the HI mass in Fig. 2c. The L_{CO}/M_{HI} ratio in this sample varies from 5×10^{-1} to 8×10^{-4} . This range in the L_{CO}/M_{HI} ratio is equal to the

range seen in galaxy type 1 to 7 (Sage 1993). At low atomic gas mass the luminosity of CO increases with the mass of the atomic gas, but the rate of increase slows down as the atomic gas mass increases. For masses of about $10^{10} M_{\odot}$ and higher there is no further increase in the luminosity of CO. This ‘observation’ depends to some degree on the data for UM274, although there is evidence for flattening from atomic gas mass of $10^9 M_{\odot}$ and higher. The D_{25} diameter of UM274 is $75''$ and if the CO density over the visible galaxy is assumed to be similar to that seen over the observed $35''$, then the CO luminosity of this galaxy will increase by about a factor of four (indicated by the arrow in Fig. 2c). This will however not remove the flattening seen in Fig. 2c. The HI data for this galaxy were obtained with a field-of-view of $4'$ (E–W) and $22'$ (N–S) (Bottinelli, Gougenheim & Paturel 1982). If we assume that the total HI gas is within $4'$ and the CO is cospatial with HI then (for a uniform CO density) the total CO luminosity of this galaxy will be a factor of about 70 higher than the observed luminosity. This will still not completely remove the flattening in Fig. 2c. It is unlikely that the CO luminosities of galaxies with HI mass greater than $10^9 M_{\odot}$ will be significantly higher than those given in Table 2 for, although the atomic gas can extend to several times the optical diameter, the CO gas is likely to be clumped around star-forming regions rather than be globally distributed like the atomic gas. The change in the CO luminosity with increasing atomic mass could be due to following reasons:

- At high atomic gas mass a large number of molecular gas clouds are formed in the galaxy and some clouds will be optically thick so that the total CO content of these clouds will not be detected. Also, if optically thick clouds shadow optically thin ones in both spatial and velocity space then a fraction of the CO in a galaxy will not be detected. High resolution spatial and velocity maps of these galaxies in molecular and atomic lines are required to explore this further.
- Another possibility for the relation in Fig. 2c may be that the star-formation in UM274 and other high HI mass galaxies in this study is independent of total atomic gas mass. The star-formation may be either a stochastic process or be triggered by events external to the galaxy e.g. by collision(s) with other galaxies or intergalactic clouds. For example, Turner, Beck & Hurt (1997) have suggested that the low CO content of NGC 5253 may be a consequence of accretion of low metallicity intergalactic gas by this galaxy. In the case of UM274, the ‘tails’ in its optical image suggest a possible collision which may have triggered a highly efficient star-formation process and increased its atomic gas mass.

3.4. CO-FIR correlation

The correlation between the CO luminosity and the FIR luminosity in BCGs has been investigated by Rickard & Harvey (1984), Young et al. (1984), Sanders & Mirabel (1985), Young et al. (1986) and others. Young et al. (1986) found that the CO luminosity is linearly correlated with FIR luminosity and that

this correlation depends on the dust temperature. The correlation is particularly tight for galaxies in well defined temperature ranges. The correlation between the CO luminosities and FIR luminosities of the current sample is shown in Fig 2d. As this sample is not large enough to divide the galaxies into dust temperature ranges, a power law was fitted to the all detections (open and filled circles) in Fig. 2d. We find a relation of the form

$$\log(L_{FIR}) = (3.31 \pm 0.84) + (0.79 \pm 0.11)\log(L_{CO})$$

The Spearman’s rho correlation coefficient for this fit is 0.88. This result is consistent with the analysis of Young et al. (1986) and it would be tempting to conclude (as has been done by Young et al. as well as by Tacconi & Young 1987) that the CO luminosities of galaxies increase linearly with their FIR luminosities. However, *this would be misleading* because the upper limits have not been included in the linear fit. If the upper limits are included the Spearman’s rho correlation coefficient drops to 0.54 implying a weaker correlation. There are large numbers of FIR-bright galaxies which are not CO bright and *the FIR luminosity of a galaxy is not a good tracer of the observed CO gas in a galaxy*. The lower CO luminosity of some FIR luminous galaxies may be due to the presence of optically thick clouds which cause shadowing. This would be consistent with the CO–HI relation discussed in Sect. 3.3.

Since massive stars are formed in dusty giant molecular clouds, the FIR luminosity is from dust heated by stars more massive than $\sim 5 M_{\odot}$ (Devereux & Young 1990). The star-formation rate is given by (Condon 1992)

$$\left[\frac{SFR(M \geq 5M_{\odot})}{M_{\odot} \text{yr}^{-1}} \right] \sim 9 \times 10^{-11} \eta^{-1} (L_{FIR}/L_{\odot})$$

The SFR obtained from the FIR luminosity will be more accurate as it will not have been affected by extinction. The SFR in these BCGs, for the FIR luminosities in Fig. 2d, range from $\sim 3 \times 10^{-4} M_{\odot} \text{yr}^{-1}$ to $179 M_{\odot} \text{yr}^{-1}$ for a dust covering factor $\eta = 1$.

At low FIR luminosities the SFR is considerably lower than that obtained from H_{β} luminosities. However, at these low FIR luminosities the dust mass is about $50 M_{\odot}$ (for a dust temperature of 45 K see Sect. 3.5) and it is possible that the dust covering factor is not as high as that assumed here (the HI covering factor could still be high).

At high FIR luminosity the SFR derived from the FIR luminosities is almost $30\times$ higher than that computed from the H_{β} luminosities, and this may be due to extinction of the latter. At these high FIR luminosities the dust mass increases to $\sim 10^7 M_{\odot}$ and the dust extinction would be expected to be greater. Also the H_{β} luminosity in Sect. 3.2 has been corrected for reddening assuming a Galactic reddening law, but it is possible that in low metallicity galaxies the form of the reddening law is different, e.g. steeper, like that observed for the LMC and SMC (Nandy et al. 1981,1982). The H_{β} luminosity will be considerably higher if a correction with a steep reddening law is applied.

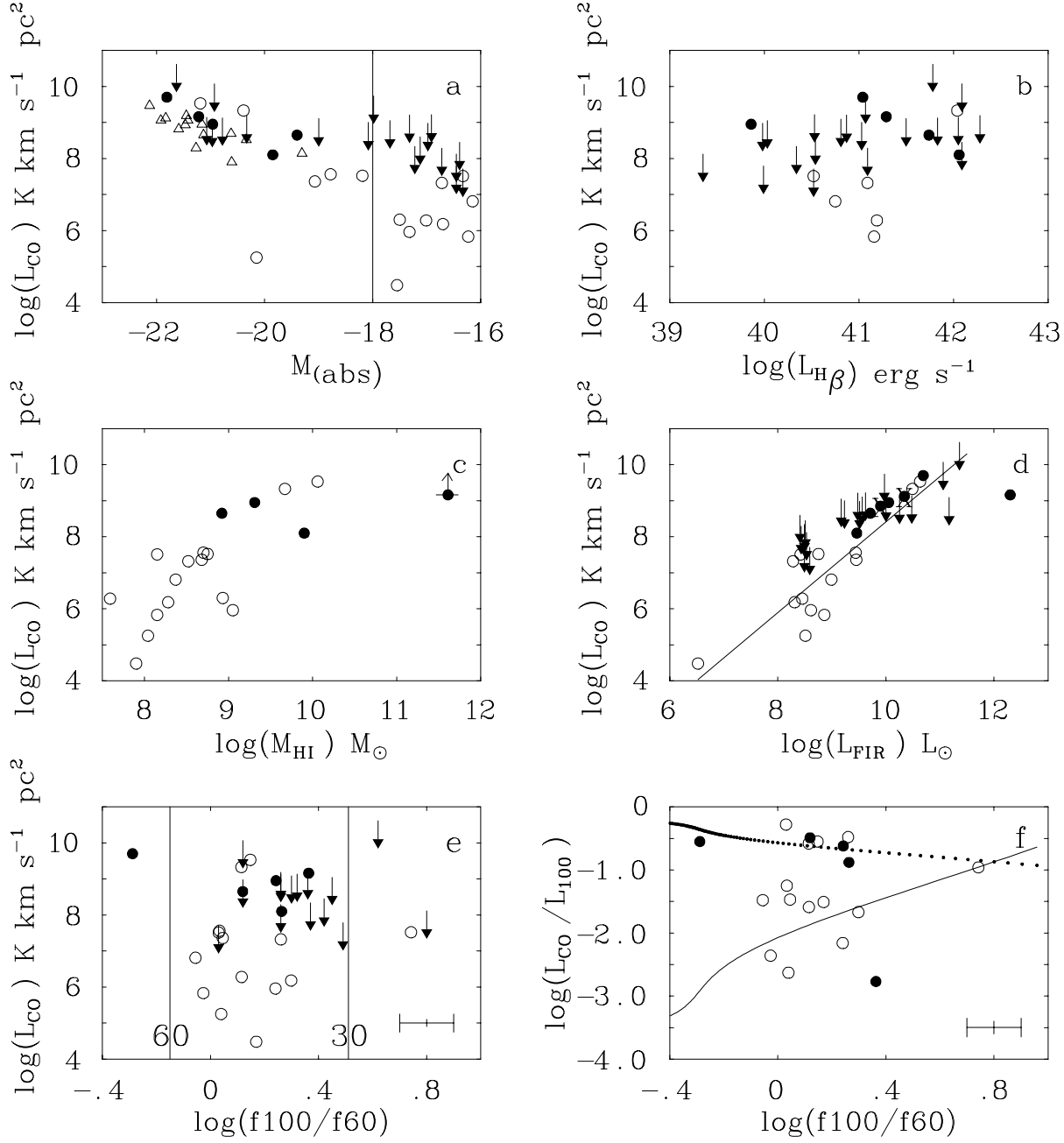


Fig. 2a–f. The correlations with CO luminosity. In these figures the filled circles are the current observations and the open circles are those of Sage et al. (1992) and Taylor, Kobulnicky & Skillman (priv. com.). In **a** the open triangles are data from Young et al. (1986). The panels show the following: **a** the correlation with absolute magnitude, **b** the correlation with H_{β} luminosity, **c** the correlation with HI mass. A typical error for the HI mass is shown by one data point (UM274) at top right. The arrow (for UM274) indicates the factor 4 increase in the CO luminosity if the complete optical galaxy had been observed for CO, **d** the correlation with FIR luminosity - the straight line is a power law fit to the observed data points and is described in Sect. 3.4, **e** the correlation with FIR colour. Here the two lines denote the colours at 30 K and 60 K (emissivity of ν^{+1}) respectively, **f** the temperature dependence of the L_{CO}/L_{100} ratio. The full line denotes a T^{-4} relation and the ‘string-of-beads’ denotes a T^{+1} relation. The 1σ error in the luminosities is of the order of the size of the open and filled circles. The 1σ error in the infrared colours is shown in the bottom right corner of figures **e** and **f**.

3.5. Temperature dependence of CO luminosity

In Fig. 2e the CO luminosity is plotted as a function of the FIR colour. The FIR colour is proportional to the temperature of the dust. No correlation is seen between these two parameters. How-

ever, if the dust and the CO gas are assumed to be in thermal equilibrium then this figure suggests that CO exists preferentially in clouds with dust temperature between 30 K and 60 K (assuming dust emissivity of ν^{+1}) However, the distribution of

data in Fig. 2e. almost certainly is due to a selection effect – the dust temperature in the selected galaxies happens to be between 30 K and 60 K. It is also possible that the (high temperature) dust detected at $60\mu\text{m}$ and $100\mu\text{m}$ and CO do not coexist.

To explore further this (lack) of correlation between CO luminosity and dust temperature we have examined the dependence of the L_{CO}/L_{100} ratio on dust temperature. Young et al. (1986) have shown that if the CO gas and dust are assumed to be in thermal equilibrium then

$$L_{CO}/L_{100} \propto T_d^{-4}$$

where L_{100} is the luminosity at $100\mu\text{m}$. In this relation dust emissivity proportional to ν^{+1} is assumed. In Fig. 2f the ratio L_{CO}/L_{100} is plotted as a function of FIR colour and the full line is the T_d^{-4} relation. A statistical fit of the relation to these data has not been attempted as the assumptions in its derivation and the errors in the observations do not warrant such detail at present. The data in Fig. 2f suggest that for about 50% of the galaxies in this sample the L_{CO}/L_{100} ratio is consistent with the T_d^{-4} relation, in agreement with the conclusions of Young et al. . However, there are equal number of galaxies in Fig. 4f for which T_d^{+1} more accurately defines the relation between L_{CO}/L_{100} and the FIR colour. If the molecular gas is in thermal equilibrium with the dust then this suggests a dust emissivity proportional to ν^{-2} in a large fraction of galaxies in this sample.

4. Conclusions

We have attempted to observe ^{12}CO in a sample 34 galaxies selected for their high star-formation rate and a large spread in absolute luminosity (or equivalently a large range in metallicity). This sample has 18 BCGs. In this sample CO has been detected in only 5 galaxies and none of these are BCGs. We have combined these observations with published observations of CO to investigate star formation in these galaxies. The following conclusions have been reached:

1. We have shown that CO is difficult to observe, or deficient in BCGs less luminous than $M_{abs} = -20$. Since absolute magnitude is correlated with metallicity, these observations confirm that CO is deficient in low metallicity galaxies.
2. The star-formation rate obtained from the $\text{H}\beta$ luminosity of a galaxy is lower than that obtained from the FIR luminosity. This may be due to the following possibilities (a) that the reddening in low metallicity galaxies is considerably steeper than the Galactic reddening law used in this analysis, or (b) that the covering factor of the neutral hydrogen gas in these galaxies is considerably different from the covering factor of dust in these galaxies.
3. The correlation between the CO luminosity and the FIR luminosity of the BCGs is rather weak i.e. FIR luminosity is not a good tracer of CO in a galaxy.
4. In some galaxies the frequently assumed ν^{+1} dust emissivity may not apply and in these galaxies a dust emissivity of ν^{-2} may be a more satisfactory explanation.

Acknowledgements. This paper was produced with facilities provided by the STARLINK Project, funded by PPARC at RAL. We would like to acknowledge the use of LEDA extragalactic database. We are grateful to the TAC of OSO for allocating observing time. EB acknowledges support from CONACyT via grant number 0460P-E.

References

- Arimoto N., Sofue Y., Tsujimoto T., 1996, PASJ, 48,275
 Arnault Ph., Casoli F., Combes F., Kunth D., 1988, A&A, 205,41
 Bottinelli L., Gougenheim L., Patrel G., 1982, A&AS, 47,171
 Brinks E., Klein U., 1988, MNRAS, 231,63P
 Condon J.J., 1992, ARA&A, 30, 575
 Davies R., 1972, IAU Symp., 44, 67
 Devereux N., Young J.S., 1990, ApJ., 359,42
 Elfhag T., Booth R.S., Höglund B., Johansson L.E.B., Sandqvist Aa., 1996, A&AS, 115,439
 Gondhalekar P.M., Morgan D.H., Dopita M., Phillips A.P., 1984, MNRAS, 208, 57
 Gondhalekar P.M., Morgan D.H., Dopita M., Ellis R.S., 1986, MNRAS, 219, 505
 Huchra J.P., 1977, ApJ, 217,928
 Israel F.P., Burton W.B., 1986, A&A, 168,369
 Israel F.P., Tacconi L.J., Baas F., 1995, A&A, 295,599
 Kobulnicky H.A., Dickey J.M., Sargent A.L., Hogg D.E., Conti P.S., 1995, AJ, 110,116
 Lonsdale C.J., Helou G., Good J.C., Rice W., 1985, *Catalogued Galaxies and Quasars Observed in the IRAS Survey* (Pasadena: Jet Propulsion Laboratory).
 MacAlpine G.M., Smith S.B., Lewis D.W., 1977a, ApJS, 35,197
 MacAlpine G.M., Smith S.B., Lewis D.W., 1977b, ApJS, 35,203
 MacAlpine G.M., Lewis D.W., 1978, ApJS, 36,587
 Nandy K., McLachlan A., Thompson G.I., Morgan D.H., Willis A.J., Wilson R., Gondhalekar P.M., Houziaux L., 1982, MNRAS, 201, 1P
 Nandy K., Morgan D.H., Willis A.J., Wilson R., Gondhalekar P.M., 1981, MNRAS, 196, 955
 Patrel et al. 1997, A&AS, 124,109
 Roberts M., Haynes M.P., 1994, ARA&A, 32, 115
 Rickard L.J., Harvey P.M., 1984, AJ, 89,1520
 Sage L.J., Salzer J.J., Loose H.-H., Henkel C., 1992, A&A, 265,19
 Sage L.J., 1993, A&A, 272,123
 Salzer J.J., MacAlpine G.M., 1988, AJ, 96,1192
 Salzer J.J., MacAlpine G.M., Boroson T.A., 1989, ApJS, 70,447
 Sanders D.B., Mirabel I.F., 1985, ApJ, 298,L31
 Searle L., Sargent W.L.W., Bagnuolo W., 1972, ApJ, 179,427
 Scoville N.Z., Young J.S., 1983, ApJ, 265,148
 Tacconi L.J., Young J.S., 1987, ApJ, 322,681
 Talbot R.J., 1980, ApJ, 235,821
 Taylor C.L., Brinks E., Grashius R.M., Skillman E.D., 1995, ApJS, 99,427
 Telesco C.M., Harper D.A., 1980, ApJ, 235,392
 Terlevich R., Melnock J., Masegosa J., Moles M., Copetti M.V.F., 1991, A&AS, 91,285
 Thuan T.X., 1983, ApJ, 268,667
 Turner J.L., Beck S.C., Hurt R.L., 1997, ApJ, 474,L11
 Wilson C.D., 1995, ApJ, 448,L97
 Young J.S., Gallagher J.S., Hunter D.A., 1984, ApJ, 276,476
 Young J.S., Schloerb F.P., Kenny J.D., Lord S.D., 1986, ApJ, 304,443